*Journal of Geosciences,* 52 (2007), 199–210 DOI: 10.3190/jgeosci.013

Original paper

# Supergene uranium mineralization from Horní Halže near Měděnec (Krušné hory Mountains), Czech Republic

Jiří SEJKORA[1*], Jiří ČEJKA[1], Vladimír ŠREIN[2]

[1] *Department of Mineralogy and Petrology, National Museum, Václavské nám. 68, 115 79 Prague 1, Czech Republic; jiri_sejkora@nm.cz*
[2] *Institute of Rock Structure and Mechanics, Academy of Sciences of the Czech Republic, V Holešovičkách 41, 182 09 Prague 8, Czech Republic*
[*] *Corresponding author*

Supergene uranium mineralization was studied at Horní Halže near Měděnec, Krušné hory Mountains, Czech Republic with the help of optical and electron scanning microscopy, X-ray powder diffraction and chemical analyses. The uranyl minerals kasolite, metatorbernite, phosphuranylite, šreinite, uranophane and uranosphaerite, together with goethite and bismutoferrite, were observed and described in detail. Chemical composition and unit-cell parameters of the minerals studied are given and compared with published data. Possible paragenetic sequences and conditions of origin are discussed.

*Keywords: uranyl, supergene minerals, uranium, unit-cell parameters, chemical composition, Horní Halže, Czech Republic*
*Received: 11 October 2007; accepted 11 December 2007; handling editor: E. Jelínek*

## 1. Introduction

Research on physico-chemical and paragenetic properties of minerals containing hexavalent uranium in the form of uranyl ion, $UO_2^{2+}$, focuses in principle in two directions. The first is the classic basic research, in which so far unknown information about uranyl minerals is obtained, inclusive their paragenesis, origin, formation and occurrence at individual localities. The second direction is concerned with the possibilities of contamination by pollutants released during weathering of natural accumulations of primary uranium minerals at shallow levels of the Earth's crust. This research potentially yields fundamental information for solution of the long-term storage of spent nuclear fuel. For this purpose are studied products of long-term weathering of natural uraninite and other $U^{4+}$-bearing mineral phases directly in the geological environment exposed to actions of exogenic factors (Finch and Ewing 1992; Wronkiewicz and Buck 1999; Shoesmith 2000; Čejka 2002 and references therein).

## 2. Occurrence

The surroundings of Horní Halže (2 km WSW of Měděnec, Krušné Hory Mts., Czech Republic) are located in the central part of the Kovářov-Halže Fold. The complicated stratigraphic and tectonic position is characterised by alternating bands of garnet mica schists, two-mica schists, migmatites and muscovite orthogneisses. In the flat-lying structures, a recurrence of allochthonous bodies of carbonate rocks, and especially barren as well as magnetite-bearing skarns, may be observed. The faults in this region are marked by dykes of Tertiary basalts and intrusions of Variscan spherulitic granite and quartz porphyry. A series of low-temperature quartz and hematite-quartz veins at Horní Halže, Kamenné, Mýtinka and other localities have been occasionally exploited as a source of decoration stone, such as zoned amethyst–chalcedony, jasper, and agate (Šrein et al. 2000).

In this region, there is a group of occurrences of radioactive mineralization, which has been a subject to an intensive exploration activity, especially in fifties and sixties of the 20th century (Šrein et al. 1996). However, no locality has reached importance of an industrial deposit and only some ore was exploited during the exploration. The most important occurrence of uranium mineralization in this region, apart from the mine No. 62 Přísečnice, are the NNW–SSE trending veins, explored by underground works starting from the Měděnec mine. They were represented by quartz–carbonate (with dolomite predominance) gangue. In the vein filling, products of arsenide, sulphoarsenide and sulphide stage prevail over products of the uraninite stage (Šrein 1978). The occurrences of uranium "blacks" in quartz veins have been investigated near Kamenná (south of Mědenec); fluorite, sphalerite, galena and pyrite were found in the association (Šrein et al. 1996).

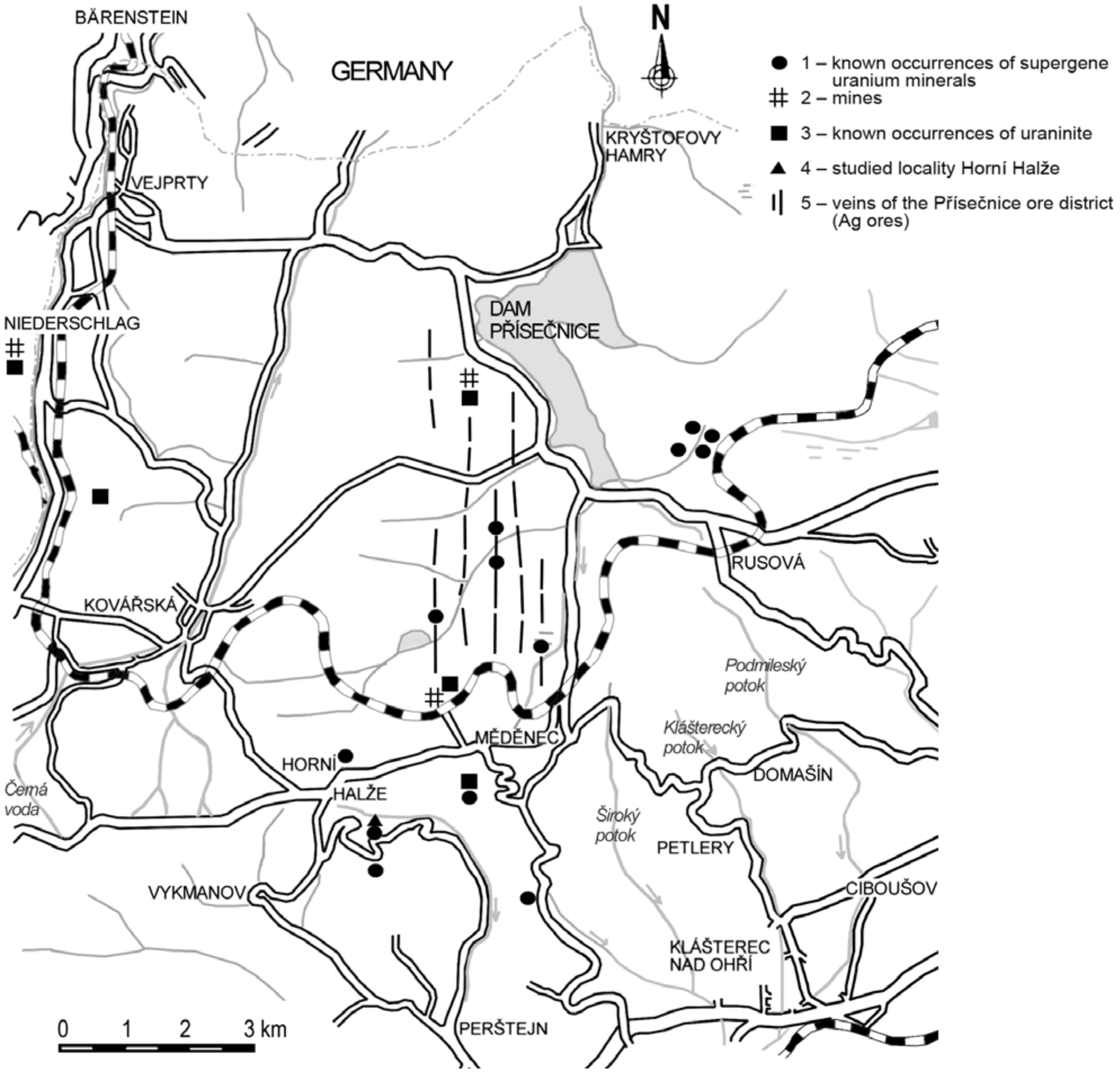

**Fig. 1** Topographic situation of the Horní Halže uranium occurrence.

The studied samples were collected at agrarian heaps of stone at the margin of the downhill run localized approximately 500 m south of the church in the village of Horní Halže (Fig. 1). In these stone heaps, both barren and magnetite skarns were observed besides quartz gangue, fragments of mica schists, migmatites, and gneisses.

In the nearest surroundings of the studied locality, occurrences of uranium mineralization were discovered in Dolní Halže village. Here exploration by the Uranium Enterprise (Zafirov and Surazhskii 1960) verified a radiometric anomaly at the intersection of a quartz vein with transversal E–W fault, which coincided with a macroscopic appearance of a uranyl silicate. In addition, in the dump material after medieval mining of iron ore north of Horní Halže, an occurrence of probable torbernite was found.

## 3. Methods applied in the study

Macro- and microscopic character of the studied mineral phases was observed in incident light using an optical microscope Nikon SMZ 1500. This microscope was also utilized for handpicking of monomineralic phases for further study. Surface morphology was studied by an electron scanning microscope Tesla BS 340 (Czech

Geological Survey, Prague) and Jeol JSM-6380 (Faculty of Science, Charles University, Prague) on gold-coated samples.

The X-ray powder diffraction patterns of the studied mineral phases were obtained using the powder diffractometer HZG4-AREM/Seifert (step-scanning, CuKα radiation, 50 kV/40 mA). To minimize the complicated shape of the background due to classic glass sample holder, the studied samples were placed on the surface of a flat silicon wafer from alcoholic suspension. The positions and the intensities of the reflections were calculated using the Pearson VII profile shape function by ZDS program package (Ondruš 1995). The measured patterns were indexed by the data calculated from the published crystal structure informations (Lazy Pulverix program – Yvon et al. 1977). Unit-cell parameters (all in $10^{-10}$ m) were refined by the program of Burnham (1962).

The studied samples have been analyzed semiquantitatively by an energy dispersive microanalyzer Link ISIS at an electron scanning microscope CamScan 4 (Faculty of Science, Charles University, Prague) at acceleration voltage 20 kV, a sample current 2.5 nA and 2 μm electron beam diameter. A natural unpolished sample surface has been utilized. Quantitative chemical analyses were carried out by means of a Cameca SX 100 electron microprobe in wavelength dispersive mode (Joint Laboratory of Electron Microscopy and Microanalysis of Masaryk University and Czech Geological Survey, Brno, performed by R. Škoda and J. Sejkora). The machine has been operated at an acceleration voltage 15 kV, a sample current 4 nA, and an electron beam diameter of 2–3 μm (2 nA and 20 μm in the case of metatorbernite). The following lines and standards were employed: Kα: Ca and Fe (andradite), S (barite), Mg (olivine), K, Si and Al (sanidine), Na (albite), Zn (ZnO), P (fluorapatite); Lα: Cu (dioptase), As (InAs); Lβ: Ba (barite); Mα: Pb (vanadinite); Mβ: U (U), Bi (Bi). Peak counting times were 20 s for main elements and 60 s for minor elements. The counting time for each background was 1/2 of the peak time. Raw intensities were converted to the concentrations using automatic PAP (Pouchou and Pichoir 1985) matrix correction software package.

## 4. Descriptions of minerals and their structural and chemical properties

All samples studied originally formed parts of a single irregular, partly rounded block with cavities up to 5×2×2 cm, and with a rim of quartz gangue, approximately 25 cm in diameter. No other occurrences of radioactive mineralization were found in the surroundings, in spite of the intesive efforts and use of a sensitive radiometer. In addition to the fine-grained (0.1–0.2 mm) and medium-grained (2–3 mm) quartz, small irregular quartz crystals 0.5–2.0 mm are present, but quartz aggregates with a distinct pitted surface due to leaching are more abundant. No additional primary mineral phases were observed. The studied samples show a low or moderate level of radioactivity.

### 4.1. Bismutoferrite, $BiFe^{3+}_2(SiO_4)_2(OH)$

Bismutoferrite forms yellow (with a shade to green and brown) very thin earthy coatings characterized by rugged surface. It is deposited on goethite in cavities and especially in small fissures of quartz gangue. Coatings are formed by very small (several μm), imperfect tabular crystals. Bismutoferrite forms coatings on an area of a few mm$^2$ in maximum. Because of its very limited amounts, it was not possible to verify its presence by X-ray diffraction. During the study of its chemical composition, substantial contents of Bi, Fe and Si were proved, with a minor admixture of Al. This information agrees with the ideal formula of bismutoferrite, $BiFe_2(SiO_4)_2(OH)$.

### 4.2. Goethite, α-$Fe^{3+}O(OH)$

Goethite was found as a prevailing phase filling cavities in the central part of the studied quartz gangue, where it forms coatings up to 1 mm thick, with hemispherical surface (Fig. 2). The aggregates consist of idiomorphic crystals only 2–4 μm in size. The observed goethite is macroscopically black-brown to black, earthy to massive with dull to earthy lustre. Goethite is the oldest supergene mineral phase in the studied association, onto which crystals of uranosphaerite and other mineral phases were deposited.

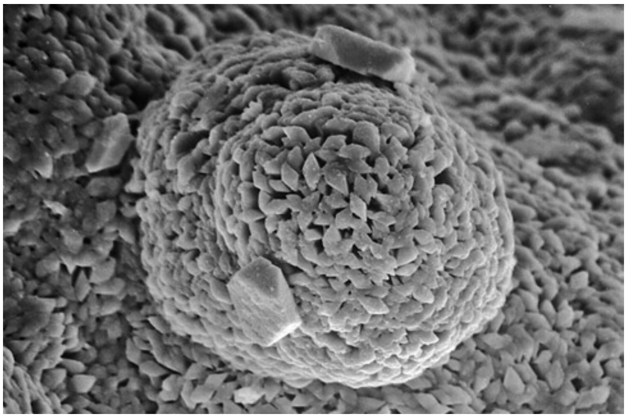

**Fig. 2** Hemispherical aggregates of goethite formed by tiny crystals (2–3 μm across) with idiomorphic uranosphaerite crystals on their surface, Horní Halže near Měděnec, SEM photo A. Gabašová, J. Sejkora (Tesla BS 340).

**Tab. 1** Unit-cell parameters of goethite (for orthorhombic space group *Pnma*)

| locality | reference | *a* | *b* | *c* | V |
|---|---|---|---|---|---|
| Horní Halže | this paper | 9.969(4) | 3.024(1) | 4.616(2) | 139.2(1) |
| synthetic | Hazemann et al. (1992) | 9.955 | 3.023 | 4.616 | 138.9 |
| Gelnica | Sejkora et al. (2001) | 9.946(3) | 3.018(1) | 4.611(1) | 138.41(6) |

The X-ray powder data of the goethite sample studied agree very well with the reference data of the PDF 2 Database and the theoretical pattern calculated from the crystal structure of goethite (Hazemann et al. 1992). The refined unit-cell parameters also agree well with other published parameters for this mineral species (Tab. 1). Only the majority content of Fe was inferred from the chemical analysis of goethite from Horní Halže. Very low, minor contents of Al, U and sporadically Bi (approximately below 0.1 wt. %) were found.

## 4.3. Kasolite, $Pb(UO_2)(SiO_4). H_2O$

In cavities of quartz gangue, kasolite forms very abundant, lightly to brightly yellow hemispherical aggregates up to 1 mm in size, formed by tiny tabular crystals. Individual, very fragile, thin tabular crystals (20–100 μm across) are intergrown to fan-shaped aggregates (Fig. 3). Kasolite was also observed together with uranophane as a part of isolated, yellow earthy pseudomorphs after primary uraninite (spherical aggregates with a diameter up to 3 mm) in quartz gangue. It also occurs as yellow to yellowish–white thin coatings up to 5×20 mm in fissures of quartz gangue. Kasolite is often intergrown with uranophane in these aggregates.

The X-ray powder data of kasolite from Horní Halže agree well with those calculated from crystal structure by Rosenzweig and Ryan (1977) in positions of individual diffraction maxima; substantial differences were observed between the measured and calculated intensities. This is probably caused by the preferred orientation of the *(h00)* type. A similar phenomenon was observed for kasolite from Jánská žíla in Příbram (Škácha and Sejkora 2001). The refined unit-cell parameters of kasolite from Horní Halže (Tab. 2) are similar to those published for this mineral from Jáchymov (Ondruš et al. 1997). Other authors presented insignificantly lower dimensions of the unit cell. The quantitative analyses of kasolite (Tab. 3) indicate a significant Pb deficiency: only 0.71–0.81 *apfu* in comparison with the ideal formula. This deficiency is balanced by notable K substitution in this structural position (0.09–0.14 *apfu*), besides minor contents of Bi, Ca, Fe, Ba and Zn. We have found no similar published information on potassium content in the structure of kasolite. On the basis of Si+P+As = 1, the empirical formula of kasolite from Horní Halže may be expressed as follows: $(Pb_{0.75}K_{0.12}Bi_{0.02}Ca_{0.01}Fe_{0.01}Ba_{0.01}Zn_{0.01})_{\Sigma 0.93}(UO_2)_{1.05}[(SiO_4)_{0.95}(PO_4)_{0.05}]_{\Sigma 1.00} . H_2O$.

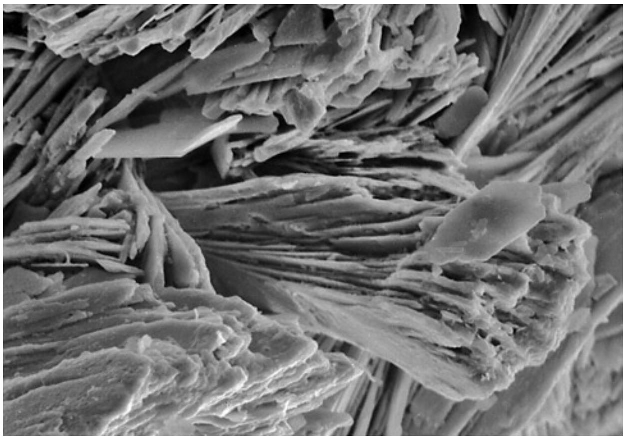

**Fig. 3** Fan-shaped aggregates (up to 50 μm) formed by thin tabular crystals of kasolite, Horní Halže near Měděnec, SEM photo A. Gabašová, J. Sejkora (Tesla BS 340).

## 4.4. Metatorbernite, $Cu(UO_2)_2(PO_4)_2.8 H_2O$

Metatorbernite was observed in cavities of quartz gangue as individual, bright green, transparent to translucent, tabular and rarely also bipyramidal crystals up to 1 mm long; there were also observed their intergrowths up to 3 mm across and sporadically also imperfectly developed leaf-shaped crystals up to 8–9 mm in length. The formation of metatorbernite in cavities of quartz gangue tempo-

**Tab. 2** Unit-cell parameters of kasolite (for monoclinic space group $P2_1/c$)

| locality | reference | *a* | *b* | *c* | *β* | V |
|---|---|---|---|---|---|---|
| Horní Halže | this paper | 6.738(2) | 6.977(2) | 13.271(4) | 104.28(3) | 604.6(4) |
| Jáchymov | Ondruš et al. (1997) | 6.730(6) | 7.022(7) | 13.307(9) | 104.90(1) | 607.7 |
| Příbram | Škácha and Sejkora (2001) | 6.707(1) | 6.950(2) | 13.258(4) | 104.20(2) | 599.1(3) |
| Shinkolobwe | Rosenzweig and Ryan (1977) | 6.704(2) | 6.932(2) | 13.252(7) | 104.2 | 597 |
| Katanga | Huynen et al. (1963) | 6.660 | 6.960 | 13.230 | 104.0 | 595.0 |
| Rýžoviště | Sejkora et al. (1994) | 6.709(4) | 6.932(4) | 13.240(7) | 104.15(4) | 597.1(6) |

**Tab. 3** Chemical composition of kasolite from Horní Halže (in wt. %)

| | mean | range (4 analyses) |
|---|---|---|
| $K_2O$ | 0.96 | 0.71 – 1.13 |
| CaO | 0.12 | 0.00 – 0.27 |
| FeO | 0.14 | 0.03 – 0.27 |
| BaO | 0.16 | 0.00 – 0.40 |
| PbO | 28.78 | 27.21 – 31.24 |
| ZnO | 0.12 | 0.00 – 0.31 |
| $Bi_2O_3$ | 0.65 | 0.47 – 0.76 |
| $SiO_2$ | 9.76 | 9.53 – 10.03 |
| $As_2O_5$ | 0.08 | 0.00 – 0.22 |
| $P_2O_5$ | 0.61 | 0.31 – 0.82 |
| $UO_3$ | 51.77 | 49.99 – 52.57 |
| $H_2O$* | 3.10 | |
| total | 96.25 | |

The $H_2O$* contents were calculated on the basis of theoretical content $H_2O$ = 1 in kasolite formula

rally overlapped with that of kasolite and uranosphaerite. However, in some places this mineral is distinctly older or younger. In fissures of quartz gangue, metatorbernite forms imperfect tables grouped into coatings on a surface up to 5×10 mm and belongs here to the youngest mineral phases.

The X-ray powder pattern of metatorbernite from Horní Halže agrees very well with the reference data of the PDF 2 Database and also with the theoretical data calculated from the crystal structure analysis data of the synthetic metatorbernite (Locock and Burns 2003). The measured pattern indicates a distinct preferred orientation of the *(h00)* type in the sample, caused by a perfect cleavage. The refined unit-cell parameters (Tab. 4) indicate a slightly increased As content in the uranyl anion sheet in metatorbernite from Horní Halže (Fig. 4). This is in agreement with its chemical analysis (Tab. 5). Phosphorus contents in tetrahedral site vary between 1.46 and 1.59 *apfu* and are accompanied by As content in the range 0.41–0.54 *apfu*. The following empirical formula was

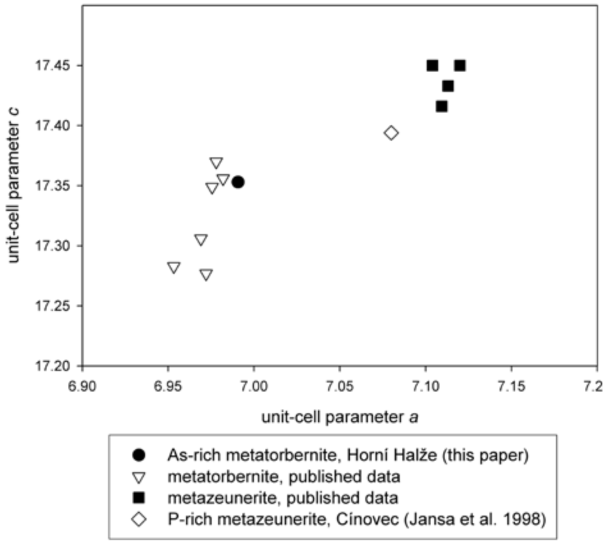

**Fig. 4** Binary plot of unit-cell parameters *a* vs. *c* for minerals of the metatorbernite–metazeunerite series (published data are given in Tab. 4).

**Tab. 5** Chemical composition of metatorbernite from Horní Halže (in wt. %)

| | mean | range (3 analyses) |
|---|---|---|
| $Na_2O$ | 0.05 | 0.00 – 0.15 |
| $K_2O$ | 0.09 | 0.02 – 0.18 |
| CaO | 0.14 | 0.10 – 0.21 |
| FeO | 0.07 | 0.00 – 0.13 |
| PbO | 0.31 | 0.00 – 0.52 |
| CuO | 8.16 | 7.97 – 8.42 |
| ZnO | 0.11 | 0.08 – 0.14 |
| $Bi_2O_3$ | 0.15 | 0.05 – 0.24 |
| $As_2O_5$ | 5.67 | 4.86 – 6.48 |
| $P_2O_5$ | 11.48 | 10.78 – 11.89 |
| $UO_3$ | 62.52 | 62.28 – 62.84 |
| $H_2O$* | 15.21 | |
| total | 103.97 | |

The $H_2O$* contents were calculated on the basis of theoretical content $H_2O$ = 8 in metatorbernite formula

**Tab. 4** Unit-cell parameters of metatorbernite (for tetragonal space group *P*4/*n*)

| mineral | locality | reference | | *a* | *c* | V |
|---|---|---|---|---|---|---|
| metatorbernite | Horní Halže | this paper | P>As | 6.9907(8) | 17.353(2) | 848.1(1) |
| metatorbernite | synt. | Locock and Burns (2003) | P | 6.9756(5) | 17.349(2) | 844.2(1) |
| metatorbernite | Schneeberg | Ross et al. (1964) | P | 6.969(1) | 17.306(5) | 840.5 |
| metatorbernite | Vathi, Greece | Stergiou et al. (1993) | P | 6.972(1) | 17.277(8) | 839.8 |
| metatorbernite | Rýžoviště | Sejkora et al. (1994) | P | 6.9533(8) | 17.283(3) | 835.6 |
| metatorbernite | Jáchymov | Ondruš et al. (1997) | P | 6.978(3) | 17.37(1) | 845.8 |
| metatorbernite | Jáchymov | Ondruš et al. (1997) | P | 6.982(1) | 17.356(5) | 846.1 |
| metazeunerite | synt. | Locock and Burns (2003) | As | 7.1094(1) | 17.416(1) | 880.3(1) |
| metazeunerite | Majuba Hill | Ross et al. (1964) | As | 7.12 | 17.45 | 884.6 |
| metazeunerite | - | Walenta (1965) | As | 7.104 | 17.45 | 880.6 |
| metazeunerite | Cínovec | Jansa et al. (1998) | As>P | 7.080(2) | 17.394(5) | 871.9 |
| metazeunerite | Jáchymov | Ondruš et al. (1997) | As | 7.113(1) | 17.433(3) | 882.0 |

calculated from the average of three point analyses on the basis of (P + As) = 2: $(Cu_{0.97}K_{0.02}Na_{0.02}Ca_{0.02}Pb_{0.01}Zn_{0.01}Fe_{0.01})_{\Sigma 1.06}(UO_2)_{2.07}[(PO_4)_{1.53}(AsO_4)_{0.47}]_{\Sigma 2.00} . 8.00H_2O$.

### 4.5. Phosphuranylite, $KCa(H_3O)_3(UO_2)_7O_4(PO_4)_4 . 8 H_2O$

Phosphuranylite forms bright yellow, in places up to orange coloured, distinctly crystalline coatings on an area up to 5×5 mm. The coatings are seen as intergrowth of thin tabular crystals (Fig. 5) having the size 10–30 μm. The individual crystals are yellowish, transparent, with an intense vitreous to adamantine lustre. Phosphuranylite does not show any fluorescence in short- or longwave UV radiation. Uranosphaerite, metatorbernite, kasolite and uranophane were observed in close association with phosphuranylite.

The measured X-ray powder data of phosphuranylite from Horní Halže (Tab. 6) agree with experimental data given for this mineral in the record 39-1350 of the PDF 2 Database with an exception of a distinct preferred orientation of the *(h00)* type. However, the data also agree with those given for yingjiangite, that may be identical with phosphuranylite and probably also isotypic dewindtite. The refined unit-cell parameters of phosphuranylite from Horní Halže (Tab. 7) agree with the data published for this mineral, however, they are also comparable with the unit-cell parameters for its Pb-analogue dewindtite, and, of course, also with yingjiangite. Phosphuranylite can be distinguished from dewindtite on the basis of comparison of their unit-cell parameters *b* and *c* (Fig. 6).

Demartin et al. (1991) studied the X-ray single crystal structure of phosphuranylite and proposed for this mineral an ideal formula $KCa(H_3O)_3(UO_2)_7O_4(PO_4)_4 . 8 H_2O$. For yingjiangite – a mineral probably identical with phosphuranylite – an ideal formula $K_2Ca(UO_2)_7(PO_4)_4(OH)_6 . 6 H_2O$ was inferred (Zhangru et al. 1990), and for probably isotypic dewindtite the formula $Pb_3[H(UO_2)_3O_2(PO_4)_2]_2 . 12 H_2O$ (Piret et al. 1990). The above given ideal formulae indicate that the chemical composition of minerals related and close to phosphuranylite has not been unambiguously solved as yet (Sejkora et al. 2003). Moreover, Demartin et al. (1991) presented in their formula of phosphuranylite oxonium ions, $H_3O^+$. The presence of $H_3O^+$ was supposed using bond-valence parameter calculations, however, such

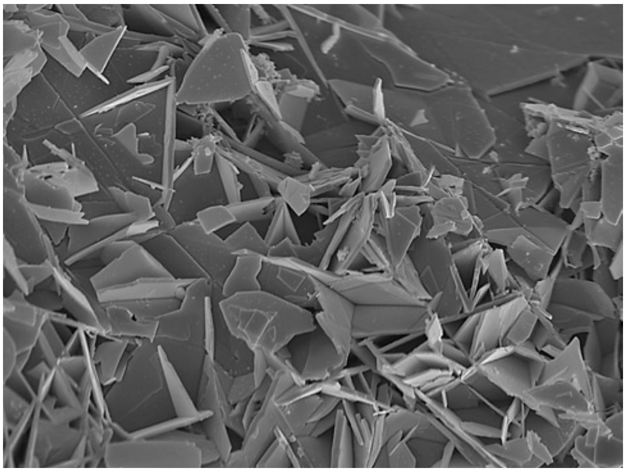

**Fig. 5** Rich aggregates formed by thin platy phosphuranylite crystals, Horní Halže near Měděnec, SEM photo J. Sejkora (Jeol JSM-6380), width of figure 45 μm.

**Tab. 6** X-ray powder diffraction pattern of phosphuranylite from Horní Halže

| *h* | *k* | *l* | $d_{obs.}$ | $I/I_o$ | $d_{calc.}$ | *h* | *k* | *l* | $d_{obs.}$ | $I/I_o$ | $d_{calc.}$ |
|---|---|---|---|---|---|---|---|---|---|---|---|
| 1 | 1 | 0 | 10.416 | 4 | 10.345 | 7 | 1 | 1 | 2.200 | 4 | 2.200 |
| 0 | 0 | 2 | 8.706 | 8 | 8.647 | 0 | 0 | 8 | 2.163 | 5 | 2.162 |
| 2 | 0 | 0 | 7.873 | 100 | 7.867 | 2 | 0 | 8 | 2.083 | 5 | 2.085 |
| 3 | 1 | 1 | 4.717 | 5 | 4.714 | 6 | 4 | 0 |  |  | 2.084 |
| 0 | 2 | 3 | 4.417 | 5 | 4.415 | 2 | 6 | 3 | 2.054 | 3 | 2.053 |
| 1 | 3 | 0 | 4.398 | 3 | 4.394 | 6 | 2 | 5 | 2.000 | 4 | 1.999 |
| 3 | 1 | 2 | 4.264 | 4 | 4.263 | 8 | 0 | 0 | 1.9661 | 6 | 1.9667 |
| 4 | 0 | 0 | 3.934 | 57 | 3.933 | 7 | 3 | 2 |  |  | 1.9647 |
| 2 | 3 | 3 | 3.858 | 8 | 3.850 | 0 | 6 | 5 | 1.9086 | 3 | 1.9084 |
| 2 | 0 | 4 | 3.790 | 5 | 3.790 | 8 | 2 | 1 | 1.8793 | 7 | 1.8765 |
| 0 | 4 | 0 | 3.436 | 5 | 3.432 | 2 | 6 | 5 | 1.8540 | 3 | 1.8546 |
| 4 | 2 | 1 | 3.347 | 9 | 3.348 | 0 | 4 | 8 | 1.8286 | 3 | 1.8293 |
| 2 | 4 | 0 | 3.146 | 7 | 3.146 | 2 | 2 | 9 | 1.8019 | 2 | 2.8013 |
| 0 | 2 | 5 | 3.090 | 8 | 3.089 | 8 | 0 | 4 | 1.7918 | 3 | 1.7902 |
| 5 | 1 | 0 | 3.068 | 6 | 3.067 | 0 | 0 | 10 | 1.7298 | 4 | 1.7295 |
| 5 | 1 | 1 | 3.022 | 4 | 3.020 | 4 | 6 | 5 | 1.7162 | 3 | 1.7170 |
| 4 | 3 | 3 | 2.931 | 5 | 2.937 | 2 | 0 | 10 | 1.6899 | 2 | 1.6891 |
| 2 | 2 | 5 | 2.876 | 8 | 2.875 | 6 | 4 | 6 |  |  | 1.6887 |
| 6 | 0 | 0 | 2.620 | 4 | 2.622 | 2 | 8 | 0 | 1.6771 | 3 | 1.6768 |
| 6 | 0 | 2 | 2.507 | 4 | 2.509 | 8 | 0 | 6 | 1.6260 | 2 | 1.6246 |
| 3 | 1 | 6 | 2.479 | 5 | 2.484 | 1 | 3 | 10 | 1.6098 | 3 | 1.6093 |
| 4 | 4 | 2 |  |  | 2.478 | 8 | 4 | 4 | 1.5879 | 3 | 1.5873 |
| 4 | 2 | 5 | 2.427 | 6 | 2.429 | 0 | 4 | 10 | 1.5431 | 3 | 1.5445 |
| 6 | 2 | 1 |  |  | 2.425 | 10 | 2 | 1 | 1.5275 | 4 | 1.5276 |
| 6 | 0 | 4 | 2.242 | 3 | 2.242 | 10 | 0 | 4 | 1.4773 | 4 | 1.4785 |
| 4 | 4 | 4 | 2.220 | 3 | 2.219 | 4 | 8 | 4 |  |  | 1.4782 |

X-ray powder diffractometer HZG4-AREM/Seifert, step-scanning 0.05°/6 s in the range 7°–66° 2θ CuKα.

**Tab. 7** Unit cell parameters of phosphouranylite and related minerals

| mineral | occurrence | reference | *a* | *b* | *c* | V |
|---|---|---|---|---|---|---|
| phosphuranylite | Horní Halže | this paper | 15.734(2) | 13.729(4) | 17.295(4) | 3736(1) |
| phosphuranylite | Sardinia | Demartin et al. (1991) | 15.899(2) | 13.740(2) | 17.300(3) | 3779 |
| phosphuranylite | Bois Noir | Demartin et al. (1991) | 15.778(3) | 13.769(2) | 17.330(3) | 3765 |
| phosphuranylite | Peveragno | Demartin et al. (1991) | 15.890(6) | 13.790(5) | 17.322(5) | 3796 |
| phosphuranylite | Zambia | Demartin et al. (1991) | 15.862(6) | 13.702(5) | 17.253(7) | 3750 |
| phosphuranylite | Margnac | Piret and Piret-Meunier (1991) | 15.835(7) | 13.724(4) | 17.324(6) | 3765 |
| phosphuranylite | – | Šaškin and Sidorenko (1975) | 15.95(2) | 13.75(2) | 17.38)4) | 3812 |
| phosphuranylite | Rýžoviště | Sejkora et al. (1994) | 15.780(7) | 13.725(8) | 17.307(8) | 3748(2) |
| phosphuranylite | Kladská | Pauliš et al. (1999) | 15.82 | 13.73 | 17.34 | 3766 |
| phosphuranylite | Jáchymov | Ondruš et al. (1997) | 15.48(2) | 13.82(2) | 17.41(4) | 3725 |
| phosphuranylite | Předbořice | Sejkora (1993) | 15.85(1) | 13.70(1) | 17.31(1) | 3759 |
| phosphuranylite | Kladská | Sejkora (1993) | 15.83(2) | 13.70(1) | 17.27(2) | 3745 |
| phosphuranylite | Chotěboř | Sejkora (1993) | 15.772(4) | 13.734(4) | 17.291(5) | 3745 |
| phosphuranylite | Horní Slavkov | Plášil et al. (2006) | 15.774(4) | 13.791(3) | 17.318(4) | 3767.5 |
| phosphuranylite | – | PDF 6-43 | 15.85 | 13.74 | 17.42 | 3794 |
| phosphuranylite | Urgeirica | Hoggart and Nuffield (1954) | 15.85(1) | 13.76(1) | 17.42((1) | 3799 |
| yingjangite | Tongbiguan | Zhangru et al. (1990) | 15.99(1) | 13.73(2) | 17.33(1) | 3804(5) |
| dewindtite | Rýžoviště | Sejkora et al. (2003) | 15.725(2) | 13.629(3) | 17.317(3) | 3711(1) |
| dewindtite | Shinkolobwe | Piret et al. (1990) | 16.031(6) | 13.605(2) | 17.264(6) | 3765 |
| dewindtite | Grury | PDF 39-1350 | 15.826(6) | 13.641(2) | 17.299(7) | 3735 |
| dewindtite | Kasolo | Hogarth and Nuffield (1954) | 16.00 | 13.66 | 17.62 | 3851 |
| dewindtite | Jáchymov | Ondruš et al. (1997) | 15.817(8) | 13.667(5) | 17.286(6) | 3737 |
| dewindtite | Jáchymov | Ondruš et al. (1997) | 15.79(3) | 13.62(1) | 17.32(1) | 3725 |
| dewindtite | Katanga | PDF 8-328 | 16.01 | 13.70 | 17.50 | 3838 |

All published data are transformed into position of orthorhombic space group *Cmcm*.

calculations are not given in the cited paper by Demartin and co-workers. The presence of $H_3O^+$ ions was proved neither in the single crystal structure analysis by Piret et al. (1990), nor in the study of the infrared spectrum of phosphuranylite (Čejka 1999). Quantitative chemical analysis of phosphuranylite from Horní Halže (Tab. 8)

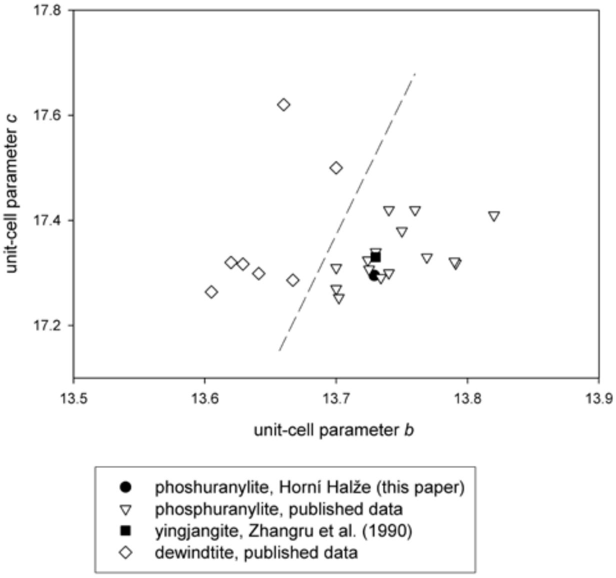

**Fig. 6** Binary plot of unit-cell parameters *b* vs. *c* for phosphuranylite, yingjangite and dewindtite (previously published data are given in Tab. 7).

**Tab. 8** Chemical composition of phosphuranylite from Horní Halže (in wt. %)

| | mean | range (5 analyses) |
|---|---|---|
| $K_2O$ | 1.90 | 1.58 – 2.02 |
| CaO | 2.02 | 1.84 – 2.18 |
| FeO | 0.04 | 0.00 – 0.10 |
| BaO | 0.42 | 0.24 – 0.50 |
| MgO | 0.08 | 0.00 – 0.18 |
| PbO | 3.24 | 2.74 – 3.77 |
| CuO | 0.16 | 0.00 – 0.42 |
| ZnO | 0.09 | 0.00 – 0.28 |
| $Al_2O_3$ | 0.03 | 0.00 – 0.06 |
| $Bi_2O_3$ | 0.81 | 0.39 – 1.31 |
| $SiO_2$ | 0.21 | 0.18 – 0.26 |
| $As_2O_5$ | 0.17 | 0.02 – 0.35 |
| $P_2O_5$ | 10.26 | 10.08 – 10.49 |
| $SO_3$ | 0.05 | 0.00 – 0.13 |
| $UO_3$ | 73.87 | 72.50 – 75.39 |
| $H_2O$* | 7.20 | |
| total | 100.53 | |

The $H_2O$* contents were calculated from the formula $KCa(H_3O)_3(UO_2)_7(PO_4)_4O_4 \cdot 8\,H_2O$ respecting the corresponding charge balance

**Tab. 9** Unit-cell parameter of šreinite and asselbornite

| mineral | occurrence | reference | *a* | V |
|---|---|---|---|---|
| šreinite | Horní Halže | Sejkora and Čejka (2007) | 15.5728(7) | 3776.6(5) |
| asselbornite | Schneeberg | Sarp et al. (1983) | 15.66 | 3840.4 |
| asselbornite | Schneeberg | Sarp et al. (1983)* | 15.6568(3) | 3838.0(2) |
| asselbornite | Schneeberg | Sejkora and Čejka (2007) | 15.613(1) | 3805.9(7) |

* unit-cell parameter refined by Sejkora and Čejka (2007) from X-ray powder pattern published by Sarp et al. (1983)

enables to conclude that the studied mineral contains, apart from K and Ca, additional cations, of which the most important is Pb (0.33–0.46 *apfu*). In the tetrahedral position, besides the dominant P (3.76–3.90 *apfu*), Si (up to 0.11), As (up to 0.08), and S (up to 0.04 *apfu*) are also present. If the formula proposed for phosphuranylite by Demartin et al. (1991) is used, chemical composition of the mineral from Horní Halže (average of 5 point analyses) may be expressed on the basis of (P + As + Si + S) = 4 by the following empirical formula: $K_{1.07}(Ca_{0.96}Pb_{0.39}Bi_{0.09}Ba_{0.07}Mg_{0.05}Cu_{0.05}Zn_{0.03}Al_{0.02})_{\Sigma 1.68}(H_3O)_{1.77}(UO_2)_{6.88}O_4[(PO_4)_{3.85}(SiO_4)_{0.09}(AsO_4)_{0.04}(SO_4)_{0.02}]_{\Sigma 4.00}$ . $8.00H_2O$.

## 4.6. Šreinite, $Pb(UO_2)_4(BiO)_3[(PO_4]_2(OH)_7$ . $4\ H_2O$

It was observed as irregular yellow coatings with a distinct orange tint, up to 0.2 mm thick, having rugged glossy surface (area up to 2×3 mm) in fissures of quartz gangue. It is lighter than the coexisting coatings and crystals of uranosphaerite, which they overgrow. Šreinite shows vitreous to subadamantine lustre, it is semi-opaque and translucent only in thin fragments, isotropic in transmitted light, with high refractive indices. No fluorescence at 254 and 366 nm of ultraviolet light was observed.

This mineral was first considered on the basis of X-ray powder pattern and semiquantitative chemical analyses as $(PO_4)$-rich asselbornite. Asselbornite is in general a very rare mineral species. Up to now it was found on a few samples from Schneeberg, Saxony, Germany (Sarp et al. 1983; Martin and Massanek 1995) and from Tirpersdorf, Vogtland, Germany (Witzke 1996). The following detailed mineralogical study proved that the natural phase from Horní Halže is unambiguously a new mineral species. This new mineral and its name were approved by *IMA* Commission on New Minerals and Mineral Names. Detailed description of this new mineral species, together with new data for analogous asselbornite, are given by Sejkora and Čejka (2007).

Šreinite is cubic, possible space group *Im*3*m*, *I*432, *Im*3 or *I*23. Its fully indexed X-ray powder diffraction pattern is given by Sejkora and Čejka (2007). The refined unit-cell parameter is compared in Tab. 9 with the data for asselbornite published by Sarp et al. (1983) and by Sejkora and Čejka (2007). According to Sejkora and Čejka (2007) average chemical composition of šreinite is BaO 0.08, CaO 0.18, MgO 0.01, PbO 7.78, $Bi_2O_3$ 29.73, $SiO_2$ 0.18, $P_2O_5$ 3.41, $As_2O_5$ 3.79, $UO_3$ 49.23, $H_2O_{calc.}$ (5.68), total (100.07) wt. %. It may be expressed on the basis of 2 atoms in tetrahedral site (P+As+Si) by the following empirical formula: $(Pb_{0.83}Ca_{0.08}Ba_{0.01}Mg_{0.01})_{\Sigma 0.93}(UO_2)_{4.10}(BiO)_{3.04}[(PO_4)_{1.15}(AsO_4)_{0.78}(SiO_4)_{0.07}]_{\Sigma 2.00}(OH)_{7.02}$ .$4\ H_2O$.

## 4.7. Uranophane, $Ca(UO_2)_2(SiO_3OH)_2.5\ H_2O$

Uranophane was found in fissures of quartz gangue as coatings on a surface up to 5×10 mm, where this mineral is intergrown with kasolite. It also forms coatings with greyish-brown shade (not typical of the mineral). It was sporadically observed as aggregates formed by needle-shaped crystals up to 5–10 µm long. As a rule, uranophane with kasolite forms a part of rare yellow powdered pseudomorphs after primary uraninite.

The X-ray powder pattern of uranophane from Horní Halže is in good agreement with the reference data from the PDF 2 Database and theoretical data calculated from the crystal structure information of this mineral (Ginderow 1988). The refined unit-cell parameters (Tab. 10) compare well with the range of published pa-

**Tab. 10** Unit-cell parameters of uranophane (for monoclinic space group $P2_1$)

| locality | reference | *a* | *b* | *c* | *β* | V |
|---|---|---|---|---|---|---|
| Horní Halže | this paper | 15.943(6) | 7.028(5) | 6.671(3) | 97.23(5) | 741.5(5) |
| Bois Noirs | Ginderow (1988) | 15.909(6) | 7.002(3) | 6.665(3) | 97.3 | 736.5 |
| Jáchymov | Ondruš et al. (1997) | 15.909(6) | 7.007(4) | 6.669(2) | 97.447(5) | 737.2 |
| Rýžoviště | Sejkora et al. (1994) | 15.968(9) | 7.024(3) | 6.680(3) | 97.12(5) | 743.4 |
| – | Stohl and Smith (1981) | 15.86(1) | 6.985(7) | 6.641(5) | 97.55(3) | 729.2 |
| – | Barinova et al. (2001) | 15.92(2) | 6.985(3) | 6.670(4) | 97.3 | 735.7 |

rameters for natural uranophane samples. Quantitative chemical study of uranophane from Halže (average from two point analyses): CaO 6.59, BaO 0.13, PbO 0.44, $Bi_2O_3$ 0.24, $SiO_2$ 12.89, $As_2O_5$ 0.34, $P_2O_5$ 1.18, $UO_3$ 70.74, $H_2O_{calc.}$ (12.48), total (105.03) wt. % leads on the basis of (2 Si + As + P) to the empirical formula: $(Ca_{1.00}Pb_{0.02}Ba_{0.01}Bi_{0.01})_{\Sigma 1.04}(UO_2)_{2.11}[(SiO_3OH)_{1.83}(PO_4)_{0.14}(AsO_4)_{0.03}]_{\Sigma 2.00} \cdot 5H_2O$. Elevated $PO_4$ contents (0.11–0.18 *apfu*) should be mentioned, because such high values have not been given for uranophane yet.

## *4.8. Uranosphaerite, $Bi(UO_2)O_2OH$*

Uranosphaerite may be related in the studied association to the relatively abundant minerals. It occurs here in two morphological types. The first is bound to cavities in the central part of the quartz vein, where it forms simple and well formed crystals having the size of 5–10 μm and pervasive subparallel intergrowths up to 0.05–0.5 mm in size (Figs 7 and 8). Crystalline aggregates up to 3 mm across were rarely observed. The morphology of crystals is consistent with monoclinic symmetry, crystal faces are often rugged and curved. Uranosphaerite crystals have dark orange to yellowish-brown colours and intense vitreous lustre. In cavities of quartz gangue, they grew on older goethite and are accompanied by light yellow kasolite and green metatorbernite. The second type is represented by the occurrence of uranosphaerite in the form of dark orange coatings in fissures of the quartz gangue. The surface of coatings is formed by small (up to 10 μm) crystals with parallel orientation. Coatings of uranosphaerite form areas up to 3×5 mm and are overgrown by light orange coatings of younger šreinite. Other mineral phases in fissures (kasolite, dewindtite, uranophane, metatorbernite) are distinctly younger and partly spatially separated from the couple uranosphaerite – šreinite.

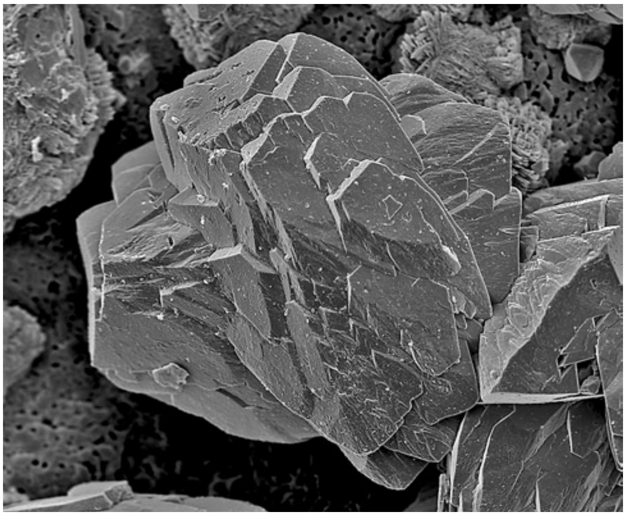

**Fig. 7** Subparallel intergrowths of uranosphaerite crystals, Horní Halže near Měděnec, SEM photo J. Sejkora (Jeol JSM-6380), width of figure 160 μm.

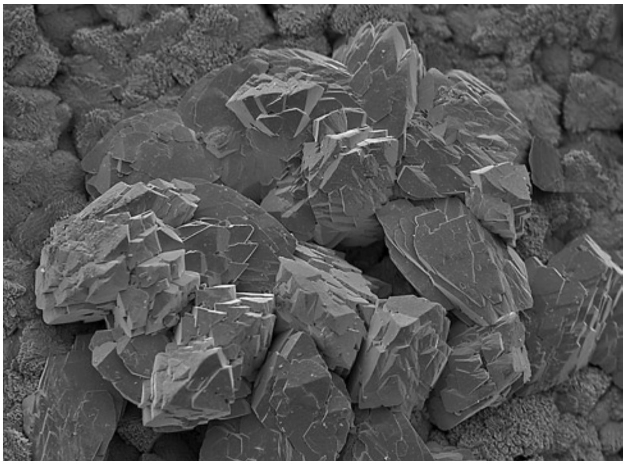

**Fig. 8** Group of uranosphaerite crystals, Horní Halže near Měděnec, SEM photo J. Sejkora (Jeol JSM-6380), width of figure 350 μm.

The crystals of uranosphaerite from Horní Halže were studied with single crystal X-ray methods (Hughes et al. 2003). The primitive monoclinic cell was found, but the crystal structure could not be solved due to poor quality of crystals. Fully indexed X-ray powder diffraction pattern of uranosphaerite from Horní Halže together with a description of its additional characteristics (especially vibrational characteristics) are given in the paper by Sejkora et al. (in print). Unit-cell parameters are compared with other published data in Tab. 11. According to Sejkora et al. (l.c.), the empirical formula $Bi_{1.02}(UO_2)_{0.99}O_{2.02}(OH)$ may be inferred from the average chemical composition of studied uranosphaerite – $Bi_2O_3$ 44.75, $UO_3$ 53.54, $H_2O$ (1.71), total (100.00) wt. %.

**Tab. 11** Unit-cell parameters of uranosphaerite (for monoclinic space group $P2_1/n$)

| locality | reference | *a* | *b* | *c* | *β* | V |
|---|---|---|---|---|---|---|
| Horní Halže | Sejkora et al. (in print) | 7.558(1) | 7.824(1) | 7.699(1) | 92.90(1) | 454.7(1) |
| Clara mine, D | Hughes et al. (2003) | 7.559(2) | 7.811(2) | 7.693(2) | 92.88(3) | 453.6(2) |
| synthetic | Hughes et al. (2003) | 7.540(3) | 7.801(3) | 7.674(3) | 92.948(7) | 450.75(1) |
| synthetic | Protas (1959) | 7.65(4) | 7.78(4) | 7.53(4) | 93(1) | 448 |

## 5. Comments on the origin of supergene uranium mineralization at Horní Halže near Měděnec

The primary mineralization of the Horní Halže occurrence was probably represented by bismuth, arsenides or rather native arsenic, pyrite and uraninite or uranium blacks in quartz gangue, which does not contain any carbonates. In comparison with the so called five-element association (known in the near surroundings, e.g. at Měděnec), the absolute deficiency in Ag, Co and Ni is characteristic of Horní Halže. Other elements present in the studied association, i.e. Ca, P and Si, were derived from altered wall rocks. The Pb contents in kasolite and šreinite are most probably of radiogenic origin with regard to the fact that no other Pb oxidic minerals were found at this locality.

The studied mineral association has been formed by intense weathering at conditions of an *in situ* supergene zone. Rich accumulations of limonite, formed by weathering of hematite and partly magnetite, associated with skarns and hematite–quartz veins, were mined in the past locally (Šrein et al. 1996). On the basis of the presence of individual mineral species and their spatial development, one can attempt to infer the character of the supergene process. It involved distinctly oxidizing conditions, neutral or slightly acidic pH (low mobility of Bi ions) and solutions of the uranylarsenate/uranylphosphate type with a moderate predominance of $(PO_4)$ over $(AsO_4)$. It is proposed that during the evolution of the studied association, the transfer of released components reached the maximum distance of several cm.

The supergene mineral association in the central porous part of the quartz gangue may be expressed as follows: quartz – goethite – uranosphaerite, kasolite, and metatorbernite. In the fissures of quartz gangue there are local older coatings of uranosphaerite and šreinite, younger aggregates of kasolite, uranophane and the youngest metatorbernite. Some changes in pH and component concentrations may be expected during formation of the individual mineral species (Langmuir 1978; Chernikov 1981; Finch and Murakami 1999). The uranyl mineral paragenetic sequence may be therefore interpreted as follows: *uranosphaerite* (very low solubility, pH approximately 2.5) – *kasolite, uranophane* (pH approximately 4.5–5.0, lower solubility of kasolite than that of uranophane) – *phosphuranylite, šreinite, metatorbernite* (pH approximately 7.5–8.5, respecting the different solubility of the mentioned mineral species).

*Acknowledgements* The authors would like to thank the Ministry of Culture of the Czech Republic, which has financially supported this work as a part of the project MK00002327201 and Grant Agency of the Academy of Sciences of the Czech Republic (project A3407401). The authors express their thank also to the late A. Gabašová (Czech Geological Survey, Prague, Czech Republic) for her help with the semiquantitative analysis of the chemical composition of the studied mineral samples and SEM photos, and to U. Kolitsch (Universität Wien, Austria) with R. Škoda (Masaryk University, Brno) for their help in laboratory treatment of studied material.

## References

Barinova AV, Rastsvetaeva RK, Sidorenko GA, Pushcharovskii DY (2001) Crystal structure of highly symmetrical alpha-uranophane. Doklady Akad Nauk 378: 201–203

Burnham ChW (1962) Lattice constant refinement. Carnegie Inst Washington Year Book 61: 132–135

Čejka J (1999) Infrared spectroscopy and thermal analysis of the uranyl minerals. Rev Mineral 38: 521–622

Čejka J (2002) Spent nuclear fuel (SNF) and immobilization of radionuclides in the structure of uranyl phases formed during its hydration-oxidation weathering in laboratory and natural conditions. Bull mineral-petrolog Odd Nár Muz (Praha) 10: 95–120 (in Czech)

Chernikov AA (1981) Behaviour of uranium in supergene zone. Nedra, Moscow, pp 1–208 (in Russian)

Demartin F, Diella V, Donzelli S, Gramaccioli CM, Pilati T (1991) The importance of accurate crystal structure determination of uranium minerals I. Phosphuranylite $KCa(H_3O)_3(UO_2)_7(PO_4)_4O_4 \cdot 8H_2O$. Acta Cryst B47: 439–446

Finch RJ, Ewing RC (1992) The corrosion of uraninite under oxidizing conditions. J Nucl Mater 190: 133–156

Finch RJ, Murakami T (1999) Systematics and paragenesis of uranium minerals. Rev Mineral 38: 91–179

Ginderow D (1988) Structure de l'uranophane alpha, $Ca(UO_2)_2(SiO_3OH)_2(H_2O)_5$. Acta Cryst C44: 421–424

Hazemann JL, Berar JF, Manceau A (1992) Rietveld studies of the aluminium–iron substitution in synthetic goethite. Phys Chem Miner 19: 25–38

Hoggart DD, Nuffield EW (1954) Studies of radioactive compounds: VII – phosphuranylite and dewindtite. Amer Miner 39: 444–447

Hughes KA, Burns PC, Kolitsch U (2003) The crystal structure and crystal chemistry of uranosphaerite, $Bi(UO_2)O_2OH$. Canad Mineral 41: 677–685

Huynen AM, Piret-Meunier J, van Meerssche M (1963) Structure de la kasolite. Bull Cl Sci (Acad Roy Belg) 49: 192–201

Jansa J, Novák F, Pauliš P, Scharmová M (1998) Supergene minerals of Sn-W deposit Cínovec, Krušné hory Mts. (Czech Republic). Bull mineral-petrolog Odd Nár Muz (Praha) 6: 83–101 (in Czech)

Langmuir D (1978) Uranium solution-mineral equilibria at low temperatures with applications to sedimentary ore deposits. Geochim Cosmochim Acta 42: 547–569

Locock AJ, Burns PC (2003) Crystal structures and synthesis of the copper-dominant members of the autunite and meta-autunite groups: torbernite, zeunerite, metatorbernite and metazeunerite. Canad Mineral 41: 489–502

Martin M, Massanek A (1995) Neufunde aus Sachsen (IV): Asselbornit aus Schneeberg/Sachsen. Lapis 20: 34–35

Ondruš P. (1995) ZDS – software for analysis of X-ray powder diffraction patterns. Version 6.01. User´s guide, pp 1–208

Ondruš P, Veselovský F, Hloušek J, Skála R, Vavřín I, Frýda J, Čejka J, Gabašová A (1997) Secondary minerals of the Jáchymov (Joachimsthal). J Czech Geol Soc 42: 3–76

Pauliš P, Ševců J, Novotný J, Rendl J (1999) Saléeite and mineral of phosphuranylite–yingjiangite series from the uranium deposit Kladská near Mariánské Lázně. Věst Čes geol Úst 74: 47–49 (in Czech)

Piret P, Piret-Meunier J (1991) Composition chimique et structure crystalline de la phosphuranylite $Ca(UO_2)(UO_2)_3(OH)_2(PO_4)_2.12H_2O$. Eur J Mineral 3: 69–77.

Piret P, Piret-Meunier J, Deliens M (1990) Composition chimique et structure cristalline de la dewindtite $Pb_3[H(UO_2)_3O_2(PO_4)_2]_2 . 12\,H_2O$. Eur J Mineral 2: 399–405

Plášil J, Sejkora J, Ondruš P, Veselovský F, Beran P, Goliáš V (2006) Supergene minerals in the Horní Slavkov uranium ore district, Czech Republic. J Czech Geol Soc 51: 149–158

Pouchou JL, Pichoir F (1985) “PAP” procedure for improved quantitative microanalysis. Microbeam Analysis 20: 104–105

Protas J (1959) Contribution à l’étude des oxydes d’uranium hydratés. Bull Soc franç Minér Crist 82: 239–272

Rosenzweig A, Ryan RR (1977) Kasolite, $Pb(UO_2)(SiO_4)(H_2O)$. Crystal Struct Comm 6: 617–621

Ross M, Evans HT, Appleman DE (1964) Studies of the torbernite minerals (II): The crystal structure of metatorbernite. Amer Miner 49: 1603–1621

Sarp H, Bertrand J, Deferne J (1983): Asselbornite, $(Pb,Ba)(UO_2)_6(BiO)_4[(As,P)O_4]_2(OH)_{12} . 3\,H_2O$. Neu Jb Miner, Mh 417–423

Sejkora J (1993) The occurrences of phosphuranylite at Czech Republic. Sbor V. min cykl sem (Horní Bečva), Ústí n. Lab., 97–99 (in Czech)

Sejkora J, Čejka J (2007) Šreinite from Horní Halže, the Krušné hory Mountains, Czech Republic, a new mineral species, its comparison with asselbornite from Schneeberg, and new data for asselbornite. Neu Jb Mineral, Abh 184: 197–206

Sejkora J, Veselovský F, Šrein V (1994) The supergene mineralization of uranium occurrence Rýžoviště near Harachov (Krkonoše Mts., Czech Republic). Acta Mus Nat Pragae, Series B, Hist Nat 50: 55–91

Sejkora J, Ďuďa R, Novotná M (2001) Minerals of oxide zone of the Krížová vein, Gelnica, the Slovenské Rudohorie Mts., Slovak Republic. Bull mineral-petrolog Odd Nár Muz (Praha) 9: 121–139 (in Czech)

Sejkora J, Čejka J, Pauliš P (2003) Rare lead uranyl phosphate–dewindtite from uranium occurrence Rýžoviště near Harrachov (Krkonoše Mts.), Bohemia, Czech Republic. Bull mineral-petrolog Odd Nár Muz (Praha) 11: 177–183 (in Czech)

Sejkora J, Čejka J, Kolitsch U (2008) Uranosphaerite from Horní Halže near Měděnec (Krušné hory Mountains, Czech Republic): its description and vibrational characteristics. Neu Jb Mineral, Abh in print

Shoesmith DW (2000) Fuel corrosion processes under waste disposal conditions. J Nucl Mater 282: 1–31

Stergiou AC, Rentzeperis PJ, Sklavounos S (1993) Refinement of the crystal structure of metatorbernite. Zeit Krist 205: 1–7

Stohl FV, Smith DK jr (1981) The crystal chemistry of the uranyl silicate minerals. Amer Miner 66: 610–625

Šaškin DP, Sidorenko GA (1975) The investigation of crystal structure of phosphuranylite. Dokl AN SSSR, 220: 1161–1164 (in Russian)

Škácha P, Sejkora J (2001) Kasolite from the Jánská vein, Březové Hory, Příbram (Czech Republic). Bull mineral-petrolog Odd Nár Muz (Praha) 9: 272–273 (in Czech)

Šrein V (1978) Study of mineralogical, geochemical and economic-geological conditions at occurrence Měděnec. Unpublished manuscript, Faculty of Science, Charles University, Prague, pp 1–115 (in Czech)

Šrein V, Bohdálek P, Šreinová B, Sejkora J (1996) A guide of mineralogical and geological localitites in the central part of the Krušné hory Mts; 30. 9.–4. 10. 1996 Měděnec. Institute of Rock Structure and Mechanics, Academy of Sciences CR, Prague, pp 1–16 (in Czech)

Šrein V, Šťastný M, Šreinová B, Bohdálek P (2000) Quartz-chalcedony veins and its young deformation. Acta Montana, Ser A 17(119): 39–43

Walenta K (1965) Die Uranglimmergruppe. Chem Erde 24: 254–275

Witzke T (1996) Neufunde aus Sachsen (V): Asselbornit, Soddyit, Konichalcit, Natrium-Zippeit, Metaschoepit und Moorhouseit. Lapis 21: 40–41

Wronkiewicz DJ, Buck E (1999) Uranium mineralogy and the geological disposal of spent nuclear fuel. Rev Mineral 38: 475–497.

Yvon K, Jeitschko W, Parthé E (1977): Lazy Pulverix, a computer program for calculation X-ray and neutron diffraction powder patterns. J Appl Cryst 10: 73–74

Zafirov AI, Surazhskii PJ (1960) Notes to geological and structural map 1:10 000 Vejprty-Přísečnice-Měděnec. Unpublished manuscript, Geofond Praha, P 18415 (in Russian)

Zhangru Ch, Yuzhu H, Xiaofa G (1990) A new mineral – yingjiangite. Acta Miner Sin 10: 102–105

## Supergenní uranová mineralizace z Horní Halže u Měděnce (Krušné hory), Česká republika

Supergenní uranová mineralizace z výskytu Horní Halže u Měděnce (Krušné hory) byla studována za využití optické a elektronové scanovací mikroskopie, rentgenové práškové difrakce a chemickým analýz na elektronovém mikroanalyzátoru. Zjištěny zde byly minerály uranylu – fosfuranylit, kasolit, metatorbernit, šreinit, uranofán a uranosférit, které jsou spolu s goethitem a bismutoferritem v práci podrobně popsány. Chemické složení a mřížkové parametry pro jednotlivé zjištěné minerální druhy jsou porovnány s publikovanými daty. Dále jsou v práci diskutovány i pravděpodobné paragenetické sekvence a podmínky této minerální asociace.